CAPACITIVE SENSING TYPE SURFACE MICROMACHINED SILICON ACCELEROMETER WITH A STIFFNESS TUNING CAPABILITY

K. Y. Park, C. W. Lee[1], H. S. Jang, Y. S. Oh[2], and B. J. Ha[2]

R&D Center, Samsung Electro-Mechanics Company,
P.O. Box 111, Suwon, Korea
Phone: +82-331-280-8082, Fax: +82-331-280-6955, Email: kyparki@samsung.co.kr
[1] Center for Noise and Vibration Control(NoViC), Department of Mechanical Engineering,
Korea Advanced Institute of Science and Technology
[2] Microsystems Lab., Samsung Advanced Institute of Technology

ABSTRACT

A novel concept surface micromachined silicon accelerometer which has a stiffness tuning capability to improve the sensor resolution is developed. The stiffness of the sensor structure is reduced by providing an electrostatic negative stiffness. By adopting the stiffness tuning, the initially stiff structure guarantees the stability of the fabrication and the reduced stiffness only along the sensing direction produces the improved resolution. In particular, one of the improved structure of this accelerometer is a branched comb-finger that senses the relative position between the mass and the electrode itself. Maintaining the same capacitance variation, it is able to achieve a larger initial gap between the mass and the electrode which fences the clash problem. The accelerometer has an active size of $650\text{x}530\mu m^2$, a thickness of polysilicon structure of $7\mu m$, and a proof mass of about $1\mu g$. Experimental results shows that the equivalent noise level of the accelerometer is improved by $30dB$ through the stiffness tuning. The accelerometer has a bandwidth of $350Hz$, a linearity of 0.3% FS, and a sensing range of $50g$.

INTRODUCTION

Since the resolution of an accelerometer is proporsional to the square of the natural frequency along the sensing direction, the natural frequency must be lowered to improve the resolution. Therefore, a bigger mass and longer beam springs should be applied. However, the compliant structure of the accelerometer causes a stiction problem in the surface micromachining process[1] and aggravates a cross sensitivity. In this paper, we adopted an electrostatic negative stiffness to lower the natural frequency along the sensing axis[2]. The stiffness of the sensor structure is reduced by providing the electrostatic negative stiffness only along sensing direction. The initially stiff sensor structure guarantees the stability of the surface micromachining process. The process stability means that the initial stiffness overcomes a surface-tension force between the structure and the substrate or interdigitated structures to each other. The stiction in the wet etching determines most of the yield of an accelerometer. An accelerometer that have been tuned with a low natural frequency has a more accurate resolution while the sensing frequency range and the dynamic range are enlarged by an electrostatic force-balancing technique[3,4]. The negative stiffness has been successfully adapted in the vibratory micro gyroscope to tune the sensing directional natural frequency[5].

The capacitive accelerometer is fabricated on a silicon wafer. The fabrication process includes the realization of a free-standing seismic mass and beam springs by means of RIE and a sacrificial PSG wet etching. Comparing with the accelerometer that has an initial stiffness, the resolution of the tuned accelerometer improved by 30dB, and yet showing good electrodynamic stability in the fabrication process and operating states.

DESIGN OF THE ACCELEROMETER

Dynamic consideration

The dynamic modeling of an accelerometer is shown in Figure 1. The accelerometer consists of a seismic mass(m) that moves along the sensing axis(y) by an external acceleration, a one dimensional spring(k) which attaches the seismic mass to the base, and a viscous damper in which the air damping is dominant in the microstructure.

0-7803-4412-X/98/$10.00 © 1998 IEEE

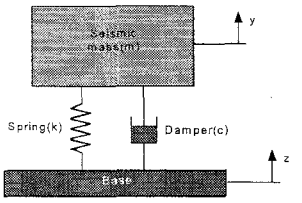

Figure 1. Dynamic model of the accelerometer

The sensing structure is a second order dynamic system whose equation of motion can be written as:

$$m\ddot{x} + c\dot{x} + kx = -m\ddot{z}, \quad x = y - z \tag{1}$$

with the following notations; m seismic mass, c damping constant, k spring constant, z displacement of the base, y the absolute displacement of the seismic mass. Here $(y\text{-}z)$ is the relative displacement between the seismic mass and the base. The transfer function between $\ddot{z}$ and x can be written as:

$$H(\omega) = \frac{x(\omega)}{\ddot{z}(\omega)} = -\frac{1}{\omega_n^2}\frac{1}{1 - r^2 + j2\varsigma r} \tag{2}$$

into the following notations; $\omega_n=(k/m)^{1/2}$ natural frequency, $r=\omega/\omega_n$ frequency ration between frequency of acceleration and natural frequency of the sensing structure, $\varsigma=c/(2(mk)^{1/2})$ damping ratio. The bandwidth of the accelerometer is far smaller than the natural frequency, so under the condition of $\omega << \omega_n$, Eqn (2) can be simplified as following:

$$H(\omega) \cong -\frac{1}{\omega_n^2} \tag{3}$$

To improve a bandwidth, a linearity and a dynamic range, a servo accelerometer with electrostatic force-balancing can has the improved bandwidth, dynamic range, and linearity as shown in Figure 2[3,4].

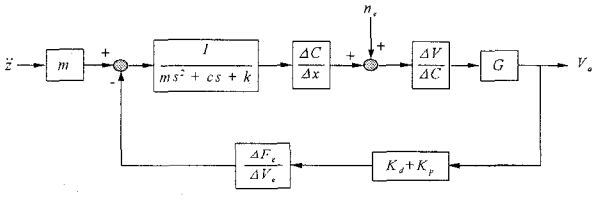

Figure 2. Block diagram of a force-balancing

Since the major sensing noise is in a capacitance to voltage converter, we insert a white capacitance noise n_e before the C-V converter($\Delta V/\Delta C$). The voltage out (V_a) which is proportional to an acceleration($\ddot{z}$) can be written as:

$$V_a = \frac{G\frac{\Delta V}{\Delta C}}{1 + G\frac{\Delta V}{\Delta C}\frac{\Delta F_e}{\Delta V_e}(K_d + K_p)}\left[H(\omega)\frac{\Delta C}{\Delta x}\ddot{z} + n_e\right] \tag{4}$$

where G is the gain of a amplifier, F_e is the force of a force-balancing, V_e is the voltage of a force-balancing, K_d is a differential feed back gain, and K_p is a proportional feed back gain. Therefore the equivalent noise level($\ddot{z}_r$) can be written as:

$$\ddot{z}_r \cong \frac{n_e}{H(\omega)\frac{\Delta C}{\Delta x}} \tag{5}$$

Finally, we can clearly find that the accelerometer which has more compliant structure has more accurate resolution if they use same displacement sensing element.

Design of a Structure

A schematic drawing of the accelerometer is shown in Figure 3. The accelerometer consists of a planar proof mass which has branched comb-fingers, the differential capacitor type position sensing electrodes to sense the relative displacement between the seismic mass and the electrodes themselves, tuning electrodes to reduce the stiffness of the structure by an electrostatic force, and four folded type beam springs. The black squares are the anchors that contacts the sensor structure to the substrate.

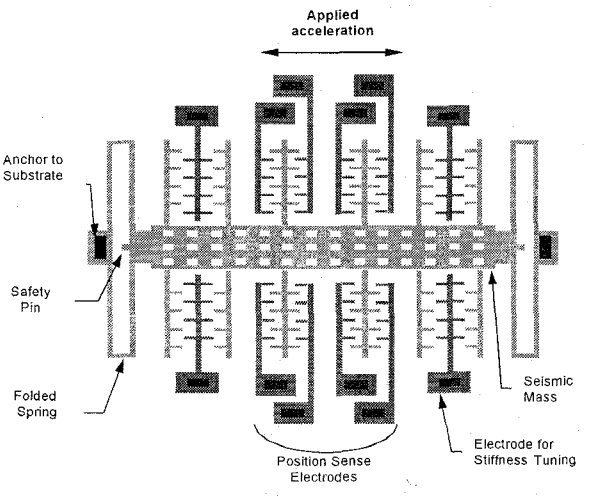

Figure 3. Schematic drawing of accelerometer

Each dimensions and shapes are designed as optimal values in the fabrication and the operating states. The area of the sensor is limited within 1 x $1mm^2$ from the cost of the production, while the thickness of the

polysilicon structure is limited to within $10\mu m$ for the stability in the fabrication process and the structural stability such as a damage of a crystal tube of LPCVD process and a residual stress.

Sensing of a relative displacement

The shapes of the electrodes that sense the gap between the seismic mass and the electrode itself are of various type. Among them, the capacitive sensing type is, to some degree, a fine method with its accuracy, frequency characteristic and simplicity of the process. The capacitive sensing element that is generally used in the surface micromachined accelerometer is a comb finger type as shown in Figure 4 (a)

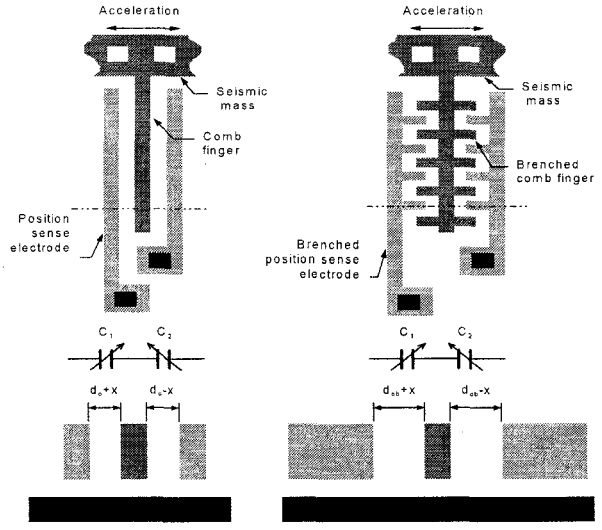

(a) Straight comb finger (b) Branched comb finger
Figure4. Position sense electrodes

The variations of the capacitance of both the capacitance C_1 and C_2 have the opposite signs. The performance of this differential capacitive sensing type electrode is improved with a small gap between the seismic mass and the electrode, and sensing area. On the other hand, in this electrode the electrostatic stability deteriorates with better sensitivity. Especially, in the accelerometer with a high resolution the instability is more serious because of its low stiffness.

In the present work, In order to overcome such clash problem we introduce a branched comb finger as shown in Figure 4 (b) and shown in detail in Figure 5. In a branched comb finger, the gap along the sensing direction d_{bo} is bigger than that of a straight comb finger, maintaining the same capacitance variation in the same occupied wafer area. So the sticking problem is solved with a bigger gap and safety pins. The g_c gap along the perpendicular axis to the sensing direction can be made much smaller than d_{bo} because the stiffness along the perpendicular axis to a sensing direction is much stiffer than the sensing direction. Actually, the gap g_c is limited by the performance of the dry etching.

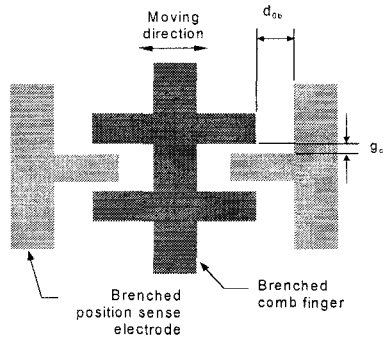

Figure 5. Detailed drawing of branched comb finger position sense electrode

However, the complexity in the shape of the branched comb finger necessitates the calculation of the capacitance variation from the displacement, obtained by an FEM electric field simulation package. Figure 6 shows the typical calculated electric displacement. In order to obtain an accurate accelerometer we find the shape of the electrode that have maximum $\Delta C/\Delta x$ under the given fabrication limits.

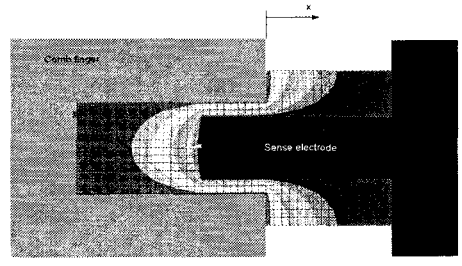

Figure 6. Result of electric field analysis(by ANSYS)

Stiffness tuning

To obtain an accelerometer with an improved resolution, we adopt an electrostatic negative stiffness to lower the natural frequency along the sensing axis[2]. The stiffness of the sensor structure can be reduced by providing the electrostatic negative stiffness only along the sensing direction. On the other hand, the initially stiff sensor structure guarantees the stability of the surface micromachining process. The potential energy U in the capacitor is

$$U = \frac{1}{2} C_t V_t^2 \qquad (6)$$

where C_t is the capacitance and V_t is the applied voltage on the capacitor. In this capacitor the electrostatic stiffness k_n is calculated as:

$$k_n = -\frac{\partial^2 U}{\partial x^2} = -\frac{1}{2} V_t^2 \frac{\partial^2}{\partial x^2} C_t . \qquad (7)$$

Generally, the electrostatic stiffness in the faced electrodes is negative, so it is often noted as a negative stiffness compared to the structural stiffness [1,5]. The widely adopted electrodes that cause the negative stiffness are straight fingers, as shown in Figure 7 (a) and the negative stiffness k'_n can be written:

$$k'_n = -\frac{2\varepsilon A_t V_t^2}{g_t^3} . \qquad (8)$$

where A_t is the area of the parallel faced electrodes and g_t is gap between both electrodes. With similarity to the position sensing, the narrow gap may cause a clash problem. In order to fence the problem, we introduce the branched finger as shown in Figure 7 (b).

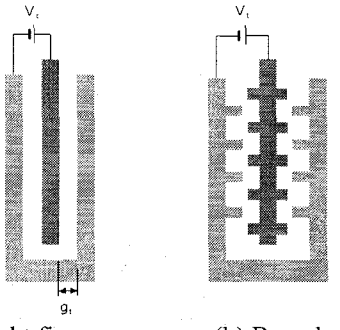

(a) Straight finger (b) Branched finger

Figure 7. Electrodes for stiffness tuning

The complexity in the shape of the branched finger necessitates the calculation of the optimal negative stiffness from the shape of electrodes, obtained by an FEM electric field simulation package like the position sensing. The optimal shape of the electrodes satisfies that the tension force is minimized and the negative stiffness is maximized, such that under the operating state the natural frequency is effectively tuned and the clash problem is fenced.

Let k_m be the structural stiffness. Then natural frequency of the tuned accelerometer f_n can be written as:

$$f_n = \sqrt{\frac{k_m + k_n}{m}} \qquad (9)$$

Like the result of the FEM field analysis, the negative stiffness is about $1N/m$ in the applied electrodes when the tuning voltage is $10Volt$. If the seismic mass is $1\mu g$ and the initial natural frequency is $5kHz$, this negative stiffness is same as the structural stiffness. So the natural frequency can be tuned with a region from its initial natural frequency to an unstable state ($k_m + k_n = 0$).

Design of a suspension

In an one input axis accelerometer, the suspension must have only one directional flexibility, no residual stress under the clamping situation and a low structural stress coupling in compression and bending stress. Considering this condition, we apply a folded beam spring. By an FEM modal analysis, we decide the dimensions of the beam spring as shown in Figure 8.

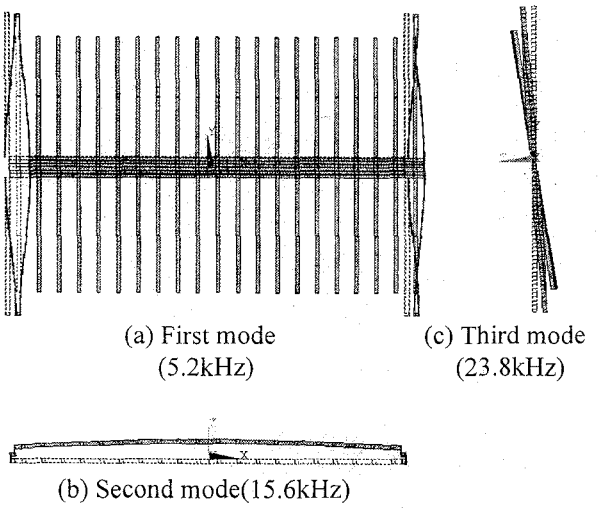

(a) First mode (5.2kHz) (c) Third mode (23.8kHz)

(b) Second mode(15.6kHz)

Figure 8. FEM modal analysis(by ANSYS)

FABRICATION

The micro structure of the accelerometer is fabricated with five mask processes. A significant advantage of this technology is that the critical features are defined with one mask, eliminating errors due to mask-to-mask misalignment. The critical features of the accelerometer are the widths of the springs, the shape of the branched comb-fingers and the tuning electrodes. These features determine the natural frequencies of the sensing mode, the sensitivity of the position sense, and the tuning performance. The cross sectional view of gyroscope is shown in Figure 9.

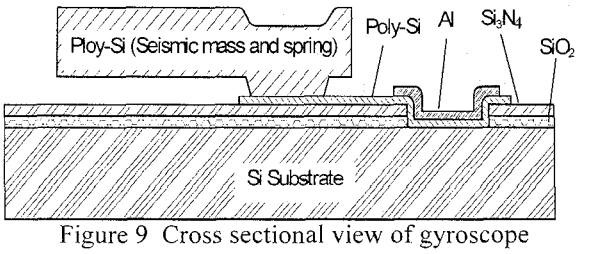

Figure 9 Cross sectional view of gyroscope

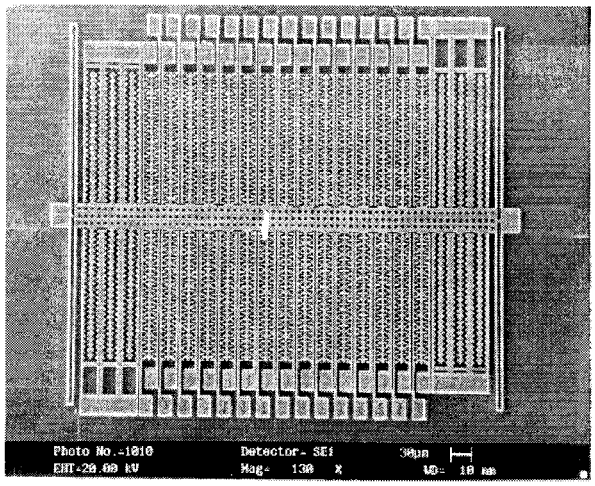

Figure 10. SEM photography of accelerometer

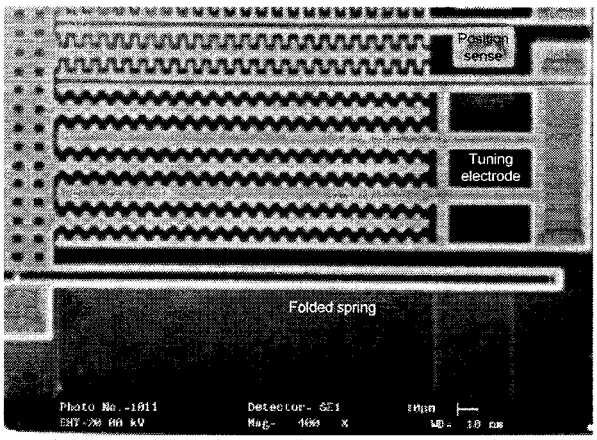

Figure 11. Branched position sense comb-fingers and tuning electrodes

The gyroscope shown in Figure 10 has an active size of 650 x 530μm^2, a thickness of the poly-silicon structure of 7μm, and a seismic mass of 1μg. Silicon wafer is used for the substrate; phosphor silicate glass for the sacrificial layer; silicon nitride and silicon oxide for the insulator; thin poly silicon film for the electric interconnection; aluminum for the wire bonding pad and the thick poly silicon for the active structure and the electrodes. The detailed shapes of the position sense electrodes, the tuning electrodes and the beam spring are shown in Figure 11.

CHARACTERIZATION

Force-balanced capacitive sensing

The circuit for the accelerometer is shown in a simplified functional block diagram in Figure 12. The circuit consists of an oscillator, charge amplifiers, a demodulator, a stiffness tuner, and a force-balancing feed back block. The moving seismic mass are driven by AC 1 $Volt_{p\text{-}p}$, 50kHz carrier. A charge signal proportional to the relative displacement between the mass and the electrodes is induced on the both sides of the position sensing electrodes[6]. The charge signals are differentially amplified after the gain balancing. The gain balancing is needed under the condition of a small unbalance of both the electrode which comes from the difference of the initial gap and the gain of the charge amp. The differentially amplified signal is rectified and low pass filtered to yield a low frequency acceleration signal. The amplified acceleration signal is fed back to the seismic mass to improve the linearity and the dynamic range. The bandwidth of the accelerometer is determined by the low pass filtering frequency of the demodulator and the feed back gain.

Calibration

The measured force-balanced frequency response of the accelerometer is shown in Figure 13. The sensitivity of the accelerometer is 39mV/g and the -3dB bandwidth is 369Hz. The frequency response of the untuned accelerometer is almost the same with that of an after stiffness tuning and the bandwidth is adjustable by an electrostatic feed back gain.

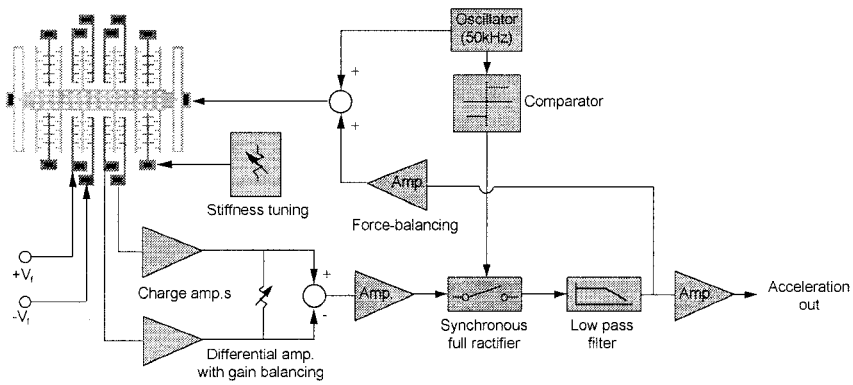

Figure 12. Schematic drawing of the force-balanced capacitive sensing

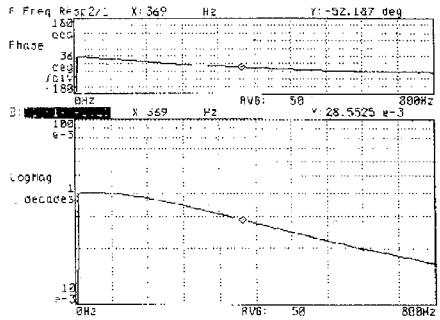

Figure 13. Frequency response

The measured nonlinearity of the accelerometer is 0.3% FS and the sensing range is 50*g*. This linearity reflects the highly linear characteristic of the electrostatic force-balancing.

The effect of the stiffness tuning is clearly shown in Figure 14 and Figure 15. Through the stiffness tuning, the equivalent noise level of the accelerometer is improved by 30*dB*, and yet maintain a good electrodynamic stability in the fabrication process and the operating states. The initial natural frequency of the accelerometer is 5.12*kHz* and that of the tuned accelerometer is about 950*Hz*.

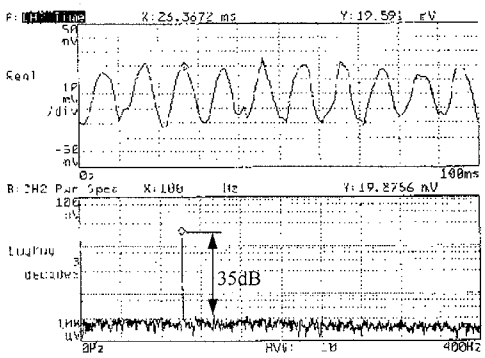

Figure 14. Output of accelerometer to a 100Hz 1g p-p sinusoidal acceleration (No stiffness tuning)

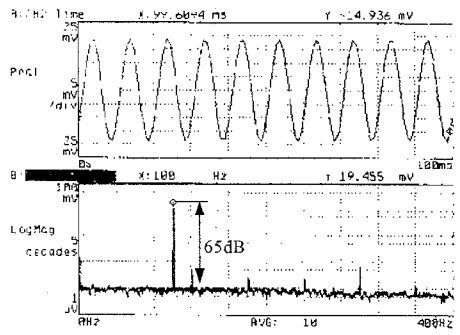

Figure 15. Output of accelerometer to a 100Hz 1g p-p sinusoidal acceleration (After stiffness tuning)

CONCLUSION

A capacitively force-balanced accelerometer with a stiffness tuning capability is successfully designed, fabricated, and calibrated. We improved the resolution of the accelerometer by 30*dB* trough the stiffness tuning and also fence the clash problem by the newly proposed electrodes.

ACKNOWLEDGEMENTS

The authors would like to thank Microsystems Lab. of Samsung-AIT, for their dedication in the fabrication and testing and the R&D center of Samsung Electro-Mechanics Company for the SEM. They also greatly acknowledge the help of the ISCR of Seoul National University, in the Si-processes.

REFERENCES

[1] Chang Liu,"A High-Yield Drying Process for Surface Microstructures using Active Levitation," *Digest of 1997 international conference on Soild-state sensors and atuators (Transducer '97)*, Chicago, USA, pp 241-244, 1997

[2] S. G. Adams, F. Bertsch, et al., "Capacitance Based Tunable Micromechanical Resonators," *Digest of 1997 international conference on Soild-state sensors and actuators (Transducer '97)*, Stockholm, Sweden, pp 438-441, 1995.

[3] K. H. L. Chau, S. R. Lewis, Y. Zhao, R. T. Howe, S. F. Bart, and R. G. Marcheselli, "An Integrated Force-Balanced Capacitive Accelerometer for Low-g Application," *Sensors and Actuators A(Physical)*, pp 472-476, 1995.

[4] L. Zimmermann, J. Ph. Ebersohl, F. Le Hung, J. P. Berry, F. Baillieu, P. Rey, B. Diem, S. Renard and P. Caillat, "Airbag Application: a Microsystem Including a Silicon Capacitive Accelerometer, CMOS Switched Capacitor Electronics and True Self-Test Capability," *Sensors and Actuators A(Physical)*, pp 190-195, 1995.

[5] K. Y. Park, C. W. Lee, Y. S. Oh and Y. H. Cho, "Laterally Oscillated and Force-balanced Micro Vibratory Gyroscope Supported by Fish Hook Shape Springs," *Digest of IEEE/ASME MEMS Workshop*, Nagoya, Japan, pp 494-499,1997.

[6] Bernhard E. Boser, "Electronics for Micromachined Inertial Sensors," *Digest of 1997 international conference on Solid-state sensors and attars (Transducer '97)*, Chicago, USA, pp 1169-1172, 1997.